

POLYNOMIAL AND RATIONAL WAVE SOLUTIONS OF KUDRYASHOV-SINELSHCHIKOV EQUATION AND NUMERICAL SIMULATIONS FOR ITS DYNAMIC MOTIONS

Turgut Ak^{1,†}, Mohammed S. Osman^{2,3} and Abdul Hamid Kara⁴

Abstract Polynomial and rational wave solutions of Kudryashov-Sinelshchikov equation and numerical simulations for its dynamic motions are investigated. Conservation flows of the dynamic motion are obtained utilizing multiplier approach. Using the unified method, a collection of exact solitary and soliton solutions of Kudryashov-Sinelshchikov equation is presented. Collocation finite element method based on quintic B-spline functions is implemented to the equation to evidence the accuracy of the proposed method by test problems. Stability analysis of the numerical scheme is studied by employing von Neumann theory. The obtained analytical and numerical results are in good agreement.

Keywords Kudryashov-Sinelshchikov equation, unified method, finite element method, collocation, solitary waves.

MSC(2010) 35A20, 76M10, 65L60.

1. Introduction

Recently, the concept of soliton has become a widely-studied topic because of its applicability in the modeling of many natural phenomena arising in different fields such as optics, physics, dynamics, fluid and biology [1, 2, 5, 7, 13, 23]. The theory of soliton has been put forward in the study of nonlinear phenomena, which makes the study of the nonlinear evolution equations (NLEEs) become an essential tool in nonlinear science.

Various analytical and numerical techniques are used to investigate the NLEEs such as the inverse scattering method [3, 4, 29], the generalized unified method [16, 17], Painlevé analysis method [24], variable separation method [30], Hirota bilinear method [26], Bäcklund transformation [27], Runge-Kutta fourth-order and

[†]The corresponding author. Email address: akturgut@yahoo.com (T. Ak)

¹Armutlu Vocational School, Yalova University, 77500 Yalova, Turkey

²Department of Mathematics, Faculty of Science, Cairo University, 12613 Giza, Egypt

³Department of Mathematics, Faculty of Applied Science, Umm Alqura University, 21955 Makkah, Saudi Arabia

⁴School of Mathematics, University of the Witwatersrand, 2050 Johannesburg, South Africa

Fourier spectral scheme [6], finite difference method [11], and the variational iteration method [25].

In this paper, we investigate and analyze the solutions of the Kudryashov-Sinelshchikov equation [21, 28] analytically and numerically by using the unified method (UM) [18, 19] and collocation method, respectively.

The Kudryashov-Sinelshchikov equation, denoted by KSE, is given by

$$u_t + \alpha uu_x + \beta u_{xxx} + \gamma (uu_{xx})_x + \sigma u_x u_{xx} = 0, \quad (1.1)$$

where α , β , γ and σ are real parameters. The KSE can be used to describe the nonlinear waves in gas-liquid mixtures in the absence of the viscosity [21]. The KSE is the generalization of the KdV when $\gamma = \sigma = 0$. For more details see [10].

Our work aims firstly to search for the solitary, soliton, and soliton rational wave solutions for the KSE by making use of the UM. Secondly, the conservation law is applied to study the invariance and the multiplier approach for the KSE. Finally, numerical simulation of the obtained results are performed on the behavior of the obtained solutions to the KSE using the quintic B-splines and the modulation instability is discussed and introduced in some figures to clarify the physical meaning for explicit and approximate solutions.

This paper is organized as follows. Section 2 constructs different types of wave solution for the KSE using the UM. Section 3 recalls some necessary preliminaries of the conservation flows for the KSE. Section 4 presents collocation finite element method for the KSE by using quintic B-splines and studies stability of the scheme. To demonstrate accuracy of the scheme, some test problems are studied and the obtained results are discussed in Section 5. Finally, conclusions are given in Section 6.

2. Exact solutions

In this section, we use the UM [18, 19] to derive exact wave solutions for Eq. (1.1). The UM classifies the solutions into two categories namely polynomial and rational wave solutions (for more details see [18, 19]).

First, we use the transformation

$$u(x, t) = u(\xi), \quad \xi = \kappa x + \nu t, \quad (2.1)$$

in Eq. (1.1) and integrating both sides with respect to ξ , we get

$$\kappa^3(\beta + \gamma u)u'' + \frac{1}{2}\sigma\kappa^3u'^2 + \frac{1}{2}\alpha\kappa u^2 + \nu u = 0, \quad u' = \frac{du}{d\xi}, \quad (2.2)$$

where the constant of integration is set to be equal zero and κ and ν are arbitrary constants.

2.1. Polynomial wave solutions

The UM asserts that the polynomial wave solutions are given by

$$u(\xi) = \sum_{j=0}^n p_j \Gamma^j(\xi), \quad (2.3)$$

and the auxiliary function $\Gamma(\xi)$ satisfies the auxiliary equation

$$(\Gamma'(\xi))^p = \sum_{j=0}^k b_j \Gamma^j(\xi), \quad p = 1, 2, \tag{2.4}$$

where p_j and b_j are real constants.

By considering the homogeneous balance between u'' and u^2 in Eq. (2.2), we get $n = 2(k - 1)$, $k \geq 1$. Here, we confine ourselves to find these solutions when $k = 2$ and $p = 1$ or $p = 2$ to obtain solitary and soliton wave solutions respectively.

2.1.1. Solitary wave solutions ($k = 2$ and $p = 1$)

Here, we find the solitary wave solutions of Eq. (2.2). From Eqs. (2.3) and (2.4) we have

$$u(\xi) = p_0 + p_1 \Gamma(\xi) + p_2 \Gamma^2(\xi), \tag{2.5}$$

$$\Gamma'(\xi) = b_0 + b_1 \Gamma(\xi) + b_2 \Gamma^2(\xi). \tag{2.6}$$

Substituting Eqs. (2.5) and (2.6) into Eq. (2.2) and equating the coefficients of $\Gamma(\xi)$ to zero (by utilizing the Mathematical software), solutions for the parameters p_i and b_i , $i = 0, 1, 2$ are presented as follows

$$p_0 = -\frac{12b_2b_0\kappa^2\beta}{\alpha - \mu^2\kappa^2\gamma}, \quad p_1 = -\frac{12b_2b_1\kappa^2\beta}{\alpha - \mu^2\kappa^2\gamma}, \quad p_2 = -\frac{12b_2^2\kappa^2\beta}{\alpha - \mu^2\kappa^2\gamma}, \tag{2.7}$$

$$\sigma = -3\gamma, \quad \nu = -\mu^2\kappa^3\beta, \quad \mu = \sqrt{b_1^2 - 4b_0b_2}.$$

Using Eq. (2.7) in Eq. (2.5) and by solving the auxiliary equation given by Eq. (2.6), we get the solution of Eq. (1.1) namely

$$u(x, t) = A \operatorname{sech}^2 [B(x - ct)], \tag{2.8}$$

where $A = \frac{3\kappa^2\mu^2\beta}{\alpha - \kappa^2\mu^2\gamma}$, $B = \frac{\kappa\mu}{2}$, $c = \kappa^2\mu^2\beta$ and $\alpha, \beta, \gamma, \kappa$ and $\mu > 0$ are arbitrary constants. Solitary wave solution of Eq. (1.1) is shown in Figure 1.

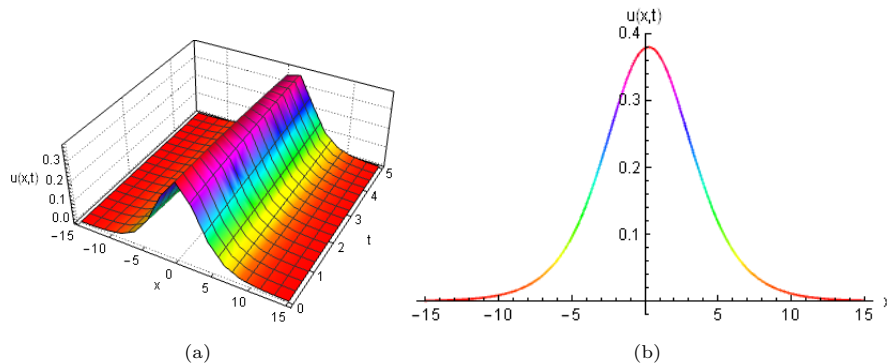


Figure 1. Solitary wave solution of Eq. (1.1) for $\alpha = 2$, $\beta = 1$, $\gamma = 0.1$, $\kappa = 1$, and $\mu = 0.5$.

2.1.2. Soliton wave solutions ($k = 2$ and $p = 2$)

To obtain the soliton wave solutions of Eq. (2.2), we put $k = 2$ and $p = 2$ in Eqs. (2.3) and (2.4) namely

$$u(\xi) = p_0 + p_1\Gamma(\xi) + p_2\Gamma^2(\xi), \quad (2.9)$$

$$\Gamma'(\xi) = \Gamma(\xi)\sqrt{b_0 + b_1\Gamma(\xi) + b_2\Gamma^2(\xi)}. \quad (2.10)$$

Using Eqs. (2.9) and (2.10) in Eq. (2.2) and by solving the obtained set of algebraic equations, we get

$$p_0 = p_1 = 0, \quad p_2 = -\frac{12b_2\kappa^2\beta}{\alpha - 4b_0\kappa^2\gamma}, \quad \nu = -4b_0\kappa^3\beta, \quad \sigma = -3\gamma, \quad b_1 = 0. \quad (2.11)$$

Using Eq. (2.11) into Eq. (2.9) and by solving the auxiliary equation given by (2.10), we get the solution of Eq. (1.1) namely

$$u(x, t) = -\frac{48b_2b_0^2 \exp[2\sqrt{b_0}\kappa(x - 4b_0\kappa^2\beta t)] \kappa^2\beta}{(\alpha - 4b_0\kappa^2\gamma) [-1 + b_0b_2 \exp(2\sqrt{b_0}\kappa(x - 4b_0\kappa^2\beta t))]^2}, \quad (2.12)$$

where α , β , γ , κ , b_2 and $b_0 > 0$ are arbitrary constants. Soliton wave solution of Eq. (1.1) is illustrated in Figure 2.

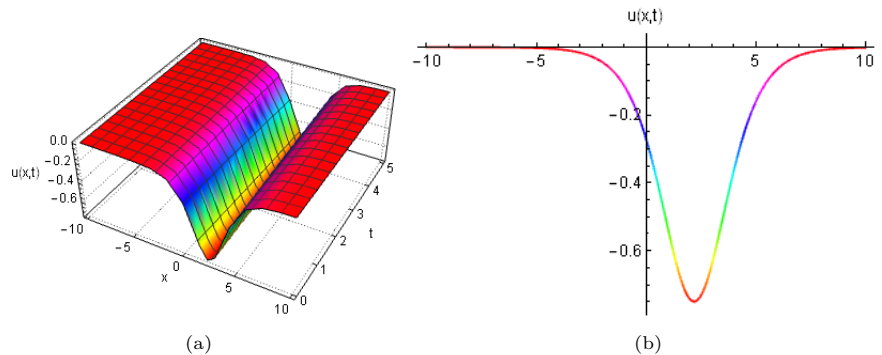


Figure 2. Soliton wave solution of Eq. (1.1) for $\alpha = -0.3$, $\beta = -0.1$, $\gamma = -0.7$, $\kappa = 0.5$, $b_0 = 0.5$, and $b_2 = -0.1$.

2.2. Rational wave solutions

To find the rational wave solutions of Eq. (1.1), we assume the solution of Eq. (2.2) as

$$u(\xi) = \frac{\sum_{i=0}^n p_i \Gamma^i(\xi)}{\sum_{j=0}^m q_j \Gamma^j(\xi)}, \quad n \geq l, \quad (2.13)$$

$$(\Gamma'(\xi))^p = \sum_{i=0}^k b_i \Gamma^i(\xi), \quad p = 1, 2 \quad (2.14)$$

where p_i , q_i and b_i are arbitrary constants. By considering the homogeneous balance between U'' and U^2 in Eq. (2.2), we get $n - m = 2(k - 1)$ and $k = 1, 2, \dots$

Here, we find those solutions when $k = 1$, $n = m$, and $p = 1$ (soliton rational solutions).

2.2.1. Soliton rational solution ($n = m = 1$ and $p = 1$)

From Eqs. (2.13) and (2.14), we have

$$u(\xi) = \frac{p_0 + p_1 \Gamma(\xi)}{q_0 + q_1 \Gamma(\xi)}, \tag{2.15}$$

$$\Gamma'(\xi) = b_0 + b_1 \Gamma(\xi).$$

Substituting Eq. (2.15) into Eq. (2.2) and by solving the obtained set of algebraic equations, we get

$$p_0 = -\frac{2b_0q_1\beta}{b_1\gamma}, \quad p_1 = -\frac{2q_1\beta}{\gamma}, \tag{2.16}$$

$$\alpha = -b_1^2\kappa^2\gamma, \quad \nu = -b_0^2\kappa^3\beta, \quad \sigma = -4\gamma.$$

Using Eq. (2.16) into Eq. (2.15), we get the solution of Eq. (1.1) namely

$$u(x, t) = -\frac{2b_1q_1\beta \exp(b_1\kappa x)}{b_1q_1\gamma \exp(b_1\kappa x) - (b_0q_1 - b_1q_0)\gamma \exp(b_1^3\kappa^3\beta t)}, \tag{2.17}$$

where $\alpha, \beta, \gamma, \kappa, q_j$ and $b_j, j = 0, 1$ are arbitrary constants. Soliton rational solution of Eq. (1.1) is drawn in Figure 3.

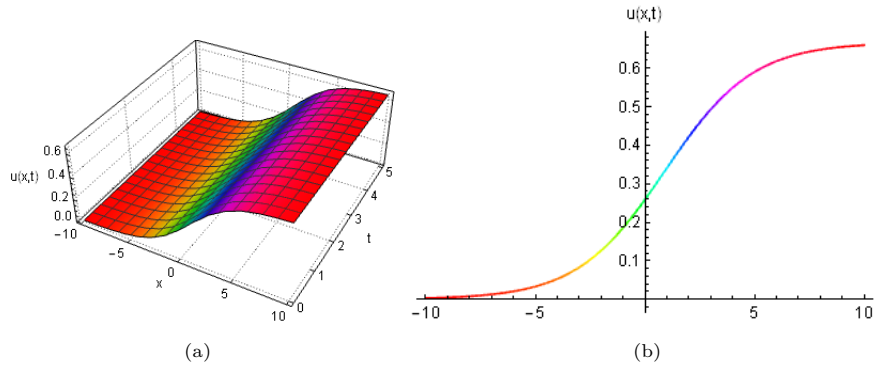


Figure 3. Soliton rational solution of Eq. (1.1) for $\alpha = -0.075, \beta = -0.1, \gamma = 0.3, \kappa = 1, b_0 = -1, b_1 = 0.5, q_0 = 0.4$ and $q_1 = -1$.

3. Conservation laws

We present some preliminaries on conservation laws that will be used in the analysis that follow.

The invariance and multiplier approach are resorted based on the well known result that the Euler-Lagrange operator annihilates a total divergence to determine conserved densities and fluxes [8]. Firstly, if (T^t, T^x) is a conserved vector corresponding to a conservation law, then

$$D_t T^t + D_x T^x = 0, \tag{3.1}$$

along the solutions of the differential equation $E(x, t, u, u_x, u_t, \dots) = 0$.

Moreover, if there exists a non-trivial differential function Q , called a “multiplier”, such that

$$\mathcal{E}_u E = 0, \quad (3.2)$$

then QE is a total divergence,

$$QE = D_t T^t + D_x T^x, \quad (3.3)$$

for some (conserved) vector (T^t, T^x) , where \mathcal{E}_u is the respective Euler-Lagrange operator. Thus, a knowledge of each multiplier Q leads to a conserved vector determined by, inter alia, a homotopy operator [9].

For a system $E_1(x, t, u, v, u_x, v_x, \dots) = 0$, $E_2(x, t, u, v, u_x, v_x, \dots) = 0$, $Q = (q^1, q^2)$, say, so that

$$q^1 E_1 + q^2 E_2 = D_t T^t + D_x T^x, \quad (3.4)$$

and

$$\mathcal{E}_{(u,v)}[D_t T^t + D_x T^x] = 0. \quad (3.5)$$

Also, the above is trivially extendable to the multi space situation so that, in the $(1 + 2)$ scenario with independent variables (t, x, y) , the conserved flow has the form (T^t, T^x, T^y) and the total divergence is $D_t T^t + D_x T^x + D_y T^y$ (equal to $QE(x, t, u, u_x, u_y, u_t, \dots)$).

Note. In this case, using the the language of forms, the conserved form (as opposed to the conserved flow) would be $T^t x - T^y x + T^x$. In each case, T^t is the *conserved density*.

It is well known that the vector fields that leave the system of differential equations invariant (generators of Lie point symmetries) contain the algebra of variational symmetries, if the latter exists [12, 14, 15, 22].

The multiplier approach, for $\sigma, \gamma \neq 0$, leads to multipliers

$$Q_1 = 1, \quad Q_2 = \left(u + \frac{\beta}{\gamma}\right)^{\sigma\gamma}. \quad (3.6)$$

The corresponding conserved flow with Q_1 has components

$$\begin{aligned} T^t &= u, \\ T^x &= \gamma u_{xx} u + \frac{1}{2} \sigma u_x^2 + \frac{1}{2} \alpha u^2 + \beta u_{xx}. \end{aligned} \quad (3.7)$$

The conserved density with Q_2 is

$$T^t = \frac{1}{\gamma + \sigma} \left[(\gamma u + \beta)^{\sigma\gamma+1} - \beta^{\sigma\gamma+1} \gamma^{-\sigma\gamma} \right]. \quad (3.8)$$

For $\sigma = 0$, the multiplier is $Q_3 = \ln(\gamma u + \beta)$ with conserved density

$$T^t = \frac{1}{\gamma} [(\gamma u + \beta) \ln(\gamma u + \beta) - \beta \ln \beta - \gamma u \ln \gamma - \gamma u]. \quad (3.9)$$

4. Numerical simulation

In this section, firstly, quintic B-spline interpolation function and its some properties are defined. The collocation finite element method is implemented to Kudryashov-Sinelshchikov equation. Quintic B-spline functions are chosen as interpolation functions. Then, stability of the applied method is analyzed using von Neumann theory.

4.1. Quintic B-splines and properties

Here, Kudryashov-Sinelshchikov equation (1.1) is studied with the physical boundary conditions $u \rightarrow 0$ as $x \rightarrow \pm\infty$, where α, β, γ and σ are constants and the subscripts t and x denote the temporal and spatial differentiations, respectively.

Firstly, the solution domain is limited over an interval $a \leq x \leq b$ to apply the numerical method. Space interval $[a, b]$ is separated into uniformly sized finite elements of length $h = \frac{b-a}{N} = (x_{m+1} - x_m)$ by the knots x_m like that $a = x_0 < x_1 < \dots < x_N = b$ for $m = 1, 2, \dots, N$.

To solve Eq. (1.1) homogeneous boundary conditions

$$\begin{aligned} u_N(a, t) &= 0, & u_N(b, t) &= 0, \\ (u_N)_x(a, t) &= 0, & (u_N)_x(b, t) &= 0, \quad t > 0 \end{aligned} \tag{4.1}$$

and

$$u(x, 0) = f(x), \quad a \leq x \leq b. \tag{4.2}$$

the initial condition are chosen as above.

$\phi_m(x)$ quintic B-spline functions at the knots x_m are defined over the interval $[a, b]$ by the following relationships for $m = -2(1)N + 2$ [20]:

$$\phi_m(x) = \frac{1}{h^5} \begin{cases} (x - x_{m-3})^5, & [x_{m-3}, x_{m-2}] \\ (x - x_{m-3})^5 - 6(x - x_{m-2})^5, & [x_{m-2}, x_{m-1}] \\ (x - x_{m-3})^5 - 6(x - x_{m-2})^5 + 15(x - x_{m-1})^5, & [x_{m-1}, x_m] \\ (x - x_{m-3})^5 - 6(x - x_{m-2})^5 + 15(x - x_{m-1})^5 - 20(x - x_m)^5, & [x_m, x_{m+1}] \\ (x - x_{m-3})^5 - 6(x - x_{m-2})^5 + 15(x - x_{m-1})^5 - 20(x - x_m)^5 + 15(x - x_{m+1})^5, & [x_{m+1}, x_{m+2}] \\ (x - x_{m-3})^5 - 6(x - x_{m-2})^5 + 15(x - x_{m-1})^5 - 20(x - x_m)^5 + 15(x - x_{m+1})^5 - 6(x - x_{m+2})^5, & [x_{m+2}, x_{m+3}] \\ 0. & \text{elsewhere} \end{cases} \tag{4.3}$$

The values of $\phi_m(x)$ and its derivative are tabulated as in Table 1. The splines $\phi_m(x)$ and its four principle derivatives vanish outside the interval $[x_{m-3}, x_{m+3}]$.

For functions defined over $[a, b]$, the set of functions $\{\phi_{-2}(x), \phi_{-1}(x), \phi_0(x), \dots, \phi_{N+1}(x), \phi_{N+2}(x)\}$ forms a basis. The approximate solution $u_N(x, t)$ is given by

$$u_N(x, t) = \sum_{j=-2}^{N+2} \phi_j(x)\delta_j(t), \tag{4.4}$$

Table 1. Quintic B-spline function and its derivatives at nodes x_m

x	x_{m-3}	x_{m-2}	x_{m-1}	x_m	x_{m+1}	x_{m+2}	x_{m+3}
$\phi_m(x)$	0	1	26	66	26	1	0
$h\phi'_m(x)$	0	-5	-50	0	50	5	0
$h^2\phi''_m(x)$	0	20	40	-120	40	20	0
$h^3\phi'''_m(x)$	0	-60	120	0	-120	60	0
$h^4\phi^{iv}_m(x)$	0	120	-480	720	-480	120	0

where $\delta_j(t)$ is time dependent parameters to be determined from the boundary and collocation conditions.

Using trial function (4.4) and quintic B-splines (4.3), the values of u , u' , u'' , u''' and u^{iv} at the knots are determined in terms of the element parameters δ_m by

$$\begin{aligned}
u_m &= u(x_m) = \delta_{m-2} + 26\delta_{m-1} + 66\delta_m + 26\delta_{m+1} + \delta_{m+2}, \\
u'_m &= u'(x_m) = \frac{5}{h}(-\delta_{m-2} - 10\delta_{m-1} + 10\delta_{m+1} + \delta_{m+2}), \\
u''_m &= u''(x_m) = \frac{20}{h^2}(\delta_{m-2} + 2\delta_{m-1} - 6\delta_m + 2\delta_{m+1} + \delta_{m+2}), \\
u'''_m &= u'''(x_m) = \frac{60}{h^3}(-\delta_{m-2} + 2\delta_{m-1} - 2\delta_{m+1} + \delta_{m+2}), \\
u^{iv}_m &= u^{iv}(x_m) = \frac{120}{h^4}(\delta_{m-2} - 4\delta_{m-1} + 6\delta_m - 4\delta_{m+1} + \delta_{m+2}),
\end{aligned} \tag{4.5}$$

where the symbols $'$, $''$, $'''$ and iv denote first, second, third and fourth differentiation with respect to x , respectively.

4.2. Implementation of the method

Substituting Eq. (4.5) into Eq. (1.1), general form of the solution approach is obtained as below.

$$\begin{aligned}
& \left(\dot{\delta}_{m-2} + 26\dot{\delta}_{m-1} + 66\dot{\delta}_m + 26\dot{\delta}_{m+1} + \dot{\delta}_{m+2} \right) + \frac{5\alpha\omega_m}{h} (-\delta_{m-2} - 10\delta_{m-1} + 10\delta_{m+1} + \delta_{m+2}) \\
& + \frac{60\beta}{h^3} (-\delta_{m-2} + 2\delta_{m-1} - 2\delta_{m+1} + \delta_{m+2}) + \frac{60\gamma\omega_m}{h^3} (-\delta_{m-2} + 2\delta_{m-1} - 2\delta_{m+1} + \delta_{m+2}) \\
& + \frac{100(\gamma+\sigma)\varpi_m}{h^3} (-\delta_{m-2} - 10\delta_{m-1} + 10\delta_{m+1} + \delta_{m+2}) = 0,
\end{aligned} \tag{4.6}$$

where

$$\omega_m = u_m = (\delta_{m-2} + 26\delta_{m-1} + 66\delta_m + 26\delta_{m+1} + \delta_{m+2}), \tag{4.7}$$

and

$$\varpi_m = \frac{h^2}{20}u_{xx} = (\delta_{m-2} + 2\delta_{m-1} - 6\delta_m + 2\delta_{m+1} + \delta_{m+2}), \tag{4.8}$$

and \cdot indicates derivative with respect to t . Here, the term u in non-linear terms uu_x and uu_{xxx} , the term $\frac{h^2}{20}u_{xx}$ in non-linear term u_xu_{xx} are taken as Eqs. (4.7) and (4.8) by assuming that the quantity u and $\frac{h^2}{20}u_{xx}$ are locally constants for the linearization technique.

If time parameters δ_i 's and its time derivatives $\dot{\delta}_i$'s in Eq. (4.6) are discretized by using the Crank-Nicolson formula and usual finite difference approximation,

respectively:

$$\delta_i = \frac{\delta_i^{n+1} + \delta_i^n}{2}, \quad \dot{\delta}_i = \frac{\delta_i^{n+1} - \delta_i^n}{\Delta t}. \quad (4.9)$$

A recurrence relationship between two time levels n and $n+1$ relating two unknown parameters δ_i^{n+1} , δ_i^n are obtained for $i = m-2, m-1, \dots, m+1, m+2$

$$\lambda_1 \delta_{m-2}^{n+1} + \lambda_2 \delta_{m-1}^{n+1} + \lambda_3 \delta_m^{n+1} + \lambda_4 \delta_{m+1}^{n+1} + \lambda_5 \delta_{m+2}^{n+1} = \lambda_5 \delta_{m-2}^n + \lambda_4 \delta_{m-1}^n + \lambda_3 \delta_m^n + \lambda_2 \delta_{m+1}^n + \lambda_1 \delta_{m+2}^n \quad (4.10)$$

where

$$\begin{aligned} \lambda_1 &= [1 - A\omega_m - (B + C\omega_m) - D\varpi_m], \\ \lambda_2 &= [26 - 10A\omega_m + 2(B + C\omega_m) - 10D\varpi_m], \\ \lambda_3 &= [66], \\ \lambda_4 &= [26 + 10A\omega_m - 2(B + C\omega_m) + 10D\varpi_m], \\ \lambda_5 &= [1 + A\omega_m + (B + C\omega_m) + D\varpi_m], \\ m &= 0, 1, \dots, N, \\ A &= \frac{5}{2h} \alpha \Delta t, \quad B = \frac{30}{h^3} \beta \Delta t, \quad C = \frac{30}{h^3} \gamma \Delta t, \quad D = \frac{50}{h^3} (\gamma + \sigma) \Delta t. \end{aligned} \quad (4.11)$$

The system (4.10) includes $(N+1)$ linear equations and $(N+5)$ unknown parameters $(\delta_{-2}, \delta_{-1}, \dots, \delta_{N+1}, \delta_{N+2})^T$. To obtain a unique solution from this system, four additional constraints are required. These are obtained from the boundary conditions by eliminating δ_{-2}, δ_{-1} and $\delta_{N+1}, \delta_{N+2}$ in the system (4.10). In this case, a matrix equation is obtained $(N+1)$ linear equations and $N+1$ unknowns $d = (\delta_0, \delta_1, \dots, \delta_N)^T$ in the following form

$$P\mathbf{d}^{n+1} = Q\mathbf{d}^n. \quad (4.12)$$

The matrices P and Q are $(N+1) \times (N+1)$ pentagonal matrices and this matrix equation (4.12) is solved by using the pentagonal algorithm. To cope with the non-linearity caused by ω_m and ϖ_m , two inner iterations are applied to the term $\delta^{n*} = \delta^n + \frac{1}{2}(\delta^n - \delta^{n-1})$ at each time step. After the initial vector $\mathbf{d}^0 = (\delta_0, \delta_1, \dots, \delta_{N-1}, \delta_N)$ is determined by using the initial condition and the following derivatives at the boundary conditions,

$$\begin{aligned} u_N(x, 0) &= u(x_m, 0), \quad m = 0, 1, 2, \dots, N \\ (u_N)_x(a, 0) &= 0, \quad (u_N)_x(b, 0) = 0, \\ (u_N)_{xx}(a, 0) &= 0, \quad (u_N)_{xx}(b, 0) = 0 \end{aligned} \quad (4.13)$$

the following matrix form of the initial vector \mathbf{d}^0 is obtained

$$W\mathbf{d}^0 = R \quad (4.14)$$

5. Results and discussion

In this section, numerical solutions of the Kudryashov-Sinelshchikov equation are considered for three problems which are including the motion of single solitary wave, interaction of two solitary waves, evolution of solitary waves with Gaussian and undular bore initial conditions.

To calculate the difference between analytical and numerical solutions and to show accuracy of the applied numerical scheme, the error norm L_2

$$L_2 = \|u^{exact} - u_N\|_2 \simeq \sqrt{h \sum_{j=1}^N |u_j^{exact} - (u_N)_j|^2}, \quad (5.1)$$

and the error norm L_∞

$$L_\infty = \|u^{exact} - u_N\|_\infty \simeq \max_j |u_j^{exact} - (u_N)_j|, \quad j = 1, 2, \dots, N, \quad (5.2)$$

are used. The Kudryashov-Sinelshchikov equation (1.1) possesses two conserved quantities as follows:

$$\begin{aligned} C_1 &= \int_a^b u dx \simeq h \sum_{j=1}^N u_j^n, \\ C_2 &= \int_a^b \left[\frac{1}{(\gamma+\sigma)} \left((\gamma u + \beta)^{\sigma\gamma+1} - \beta^{\sigma\gamma+1} \gamma^{-\sigma\gamma} \right) \right] dx \simeq h \sum_{j=1}^N \left[\frac{1}{(\gamma+\sigma)} \left((\gamma u_j^n + \beta)^{\sigma\gamma+1} - \beta^{\sigma\gamma+1} \gamma^{-\sigma\gamma} \right) \right]. \end{aligned} \quad (5.3)$$

The conserved quantities C_1 and C_2 are calculated to check the conservation of some quantities during the wave motion.

5.1. The motion of single solitary wave

The single solitary wave solution of the Kudryashov-Sinelshchikov equation (1.1) is given by

$$u(x, t) = A \operatorname{sech}^2 [B(x - ct)], \quad (5.4)$$

where $A = \frac{3\beta\kappa^2\mu^2}{\alpha - \gamma\kappa^2\mu^2}$, $B = \frac{\kappa\mu}{2}$ and $c = \beta\kappa^2\mu^2$. Note that, α , β , γ , $\sigma = -3\gamma$, κ and μ are arbitrary constants. During the calculation, we get the initial condition as

$$u(x, 0) = A \operatorname{sech}^2 [Bx]. \quad (5.5)$$

with the boundary conditions $u \rightarrow 0$ as $x \rightarrow \pm\infty$.

To show the motion of the single solitary wave solution numerically over the interval $x \in [-60, 40]$, the parameters are chosen as $\alpha = 1.5$, $\beta = 1.7$, $\gamma = 0.8$, $\sigma = -2.4$, $c = 0.425$, $\kappa = 1$, $\mu = 0.5$ for $h = \Delta t = 0.1$ and $h = \Delta t = 0.025$, respectively. The solitary wave has *amplitude* = 0.98 for these parameters. The error norms and conserved quantities are calculated up to time $t = 20$ for different values of h and Δt . The obtained results are tabulated in Table 2. It can be seen from the Table 2 that L_2 and L_∞ error norms are found to be satisfactorily small and the conserved quantities are pretty much unchanged as the time progresses. The percentage of relative changes of C_1 and C_2 are found to be 5.920×10^{-5} and 6.488×10^{-6} for $h = \Delta t = 0.1$; 4.689×10^{-5} and 4.720×10^{-6} for $h = \Delta t = 0.025$, respectively. It is observed from the Table 2 that numerical results are better and more accurate for small values of h and Δt . If we observe Figure 4(a), we find

bell shaped solitary wave solutions produced. Also, contour line for motion of the single solitary wave can be seen in Figure 4(b). As it can be clearly seen from the figures, the solitary wave moves to the right at a constant speed. As expected, its amplitude and shape are preserved as time passes. On the other hand, error graphs are plotted for different values of h and Δt in Figure 5.

Table 2. Conserved quantities and error norms for motion of the single solitary wave

	t	C_1	C_2	$L_2 - Error$	$L_\infty - Error$
$h = \Delta t = 0.1$	0.0	7.8461558037	-12.3622499053	0.000000000000	0.000000000000
	2.5	7.8461557523	-12.3622499493	1.367597×10^{-5}	5.729885×10^{-6}
	5.0	7.8461557779	-12.3622499622	2.196199×10^{-5}	1.012597×10^{-5}
	7.5	7.8461553075	-12.3622500428	3.096934×10^{-5}	1.417086×10^{-5}
	10.0	7.8461554338	-12.3622500188	4.000045×10^{-5}	1.803005×10^{-5}
	12.5	7.8461531619	-12.3622503907	4.983849×10^{-5}	2.192837×10^{-5}
	15.0	7.8461573181	-12.3622496956	5.860834×10^{-5}	2.505833×10^{-5}
	17.5	7.8461518803	-12.3622505934	6.581260×10^{-5}	2.693506×10^{-5}
	20.0	7.8461511588	-12.3622507074	7.413800×10^{-5}	2.959083×10^{-5}
	t	C_1	C_2	$L_2 - Error$	$L_\infty - Error$
$h = \Delta t = 0.025$	0.0	7.8461455100	-12.3522259633	0.000000000000	0.000000000000
	2.5	7.8461454628	-12.3522259731	2.413295×10^{-6}	1.076032×10^{-6}
	5.0	7.8461455773	-12.3522259455	3.485312×10^{-6}	1.460035×10^{-6}
	7.5	7.8461453565	-12.3522259743	4.272701×10^{-6}	1.857019×10^{-6}
	10.0	7.8461452507	-12.3522259868	5.791756×10^{-6}	2.159832×10^{-6}
	12.5	7.8461444368	-12.3522261185	8.413219×10^{-6}	3.713176×10^{-6}
	15.0	7.8461449845	-12.3522260257	1.231469×10^{-5}	5.834287×10^{-6}
	17.5	7.8461430957	-12.3522263379	1.707483×10^{-5}	8.178540×10^{-6}
	20.0	7.8461418312	-12.3522265463	2.265791×10^{-5}	1.063514×10^{-5}

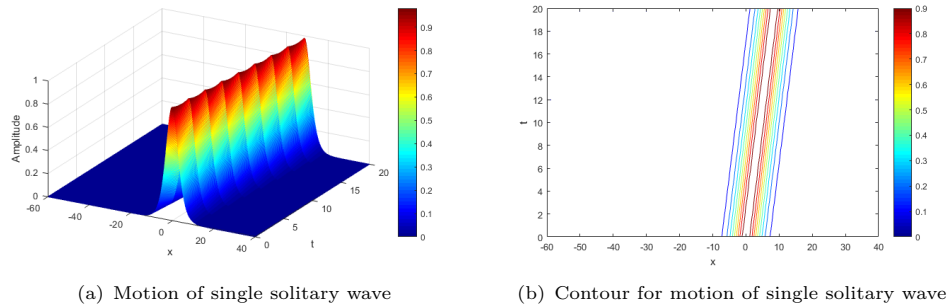


Figure 4. Motion of single solitary wave and its contour

5.2. Interaction of two solitary waves

Secondly, the interaction of two solitary waves advancing in the same direction is considered by using the initial condition given by the linear sum of two well separated solitary waves having different amplitudes

$$u(x, 0) = \sum_{i=1}^2 A_i \text{sech}^2 [B_i (x - x_i)], \tag{5.6}$$

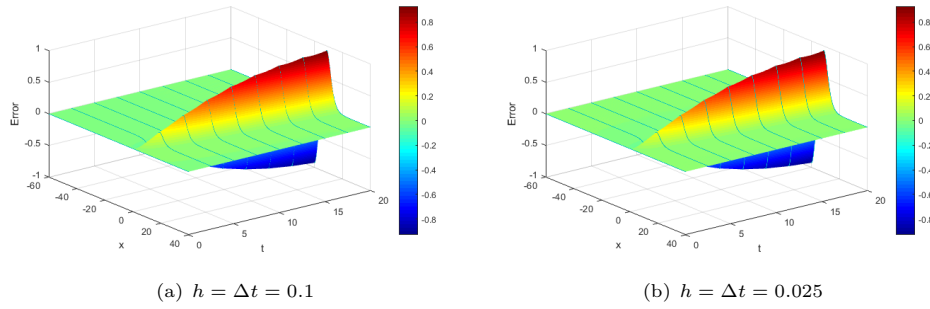


Figure 5. Error norms for motion of the single solitary wave

where $A_i = \frac{3\beta\kappa^2\mu_i^2}{\alpha-\gamma\kappa^2\mu_i^2}$, $B_i = \frac{\kappa\mu_i}{2}$ and $c_i = \beta\kappa^2\mu_i^2$ for $i = 1, 2$. Also, x_i is arbitrary constant.

To show simulation over the interval $x \in [-100, 100]$, the parameters are taken to be $\alpha = 1.5$, $\beta = 1.7$, $\gamma = 0.8$, $\sigma = -2.4$, $\kappa = 1$, $\mu_1 = 0.7$, $\mu_2 = 0.5$, $c_1 = 0.833$, $c_2 = 0.425$, $x_1 = -35$, $x_2 = 10$ for $h = \Delta t = 0.1$ and $h = 0.025$, $\Delta t = 0.01$, respectively. During the interaction of two solitary waves, the values of the two conserved quantities C_1 and C_2 can be seen in Table 3 for different values of h and Δt . It is seen that the obtained values of the conserved quantities remain more constant sensibly for small values of h and Δt . While interacting, the travelling wave profiles can be seen in Figure 6(a). Contour line for interaction of two solitary waves is depicted in Figure 6(b). It is clear from the figures that, the large solitary wave is located to the left of the small solitary wave at the beginning of the calculation. With increasing time, the large solitary wave catches up the small wave until $t = 30$, then the small solitary wave is absorbed. The overlap process continues until $t = 60$, then the large solitary wave has overtaken the small solitary wave and the separation process begins. At time $t = 70$, the interaction is completed and the large solitary wave has separated completely. At the end of this process, solitary waves preserve their original amplitudes and shapes.

Table 3. Conserved quantities for the interaction of two solitary waves

t	$h = 0.1$	$\Delta t = 0.1$	$h = 0.025$	$\Delta t = 0.01$
	C_1	C_2	C_1	C_2
0	20.7343903136	-24.4006865491	0.0003587567	-6.6868057075
10	20.7344125274	-24.4005864401	0.0001414754	-6.6868417960
20	20.7344271657	-24.3998924146	0.0000488112	-6.6868571878
30	20.7344310727	-24.3957076573	0.0000875714	-6.6868507448
40	20.7343425231	-24.3832055971	0.0002023407	-6.6868317004
50	20.7344385138	-24.3896941137	0.0001342899	-6.6868429859
60	20.7343773107	-24.3989882874	0.0000622223	-6.6868549558
70	20.7344018243	-24.4006154476	0.0000759852	-6.6868526692
80	20.7343755930	-24.4007677831	0.0000338496	-6.6868596667

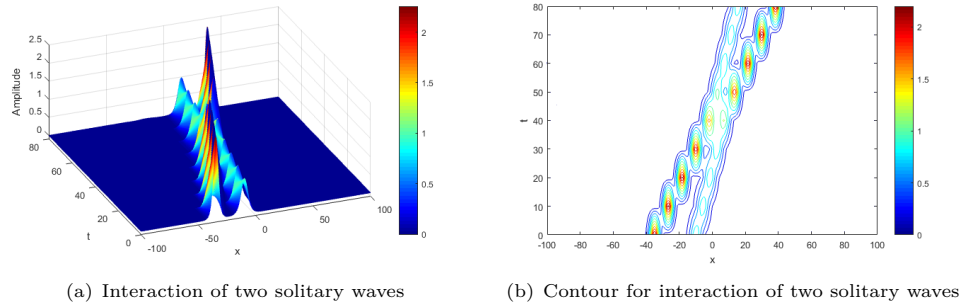


Figure 6. Interaction of two solitary waves and its contour

5.3. Evolution of solitary waves

As a last test problem, Gaussian and undular bore initial conditions are studied to show birth of solitary waves.

5.3.1. Gaussian initial condition

Evolution of a train of solitary waves is studied on Kudryashov-Sinelshchikov equation using the Gaussian initial condition

$$u(x, 0) = \exp(-x^2), \quad (5.7)$$

and boundary condition

$$u(-200, t) = u(100, t) = 0, \quad t > 0. \quad (5.8)$$

Parameters are taken as $\alpha = 1.5$, $\beta = 1.7$, $\gamma = 0.8$, $\sigma = -2.4$, $c = 0.425$, $\kappa = 1$, $\mu = 0.5$ for $h = \Delta t = 0.1$ and $h = 0.08$, $\Delta t = 0.05$ respectively. The numerical calculations are done until time $t = 60$. The values of the two conserved quantities of motion according to space and time steps are presented in Table 4. Here, especially the conserved quantity C_2 is preserved better for small values of h and Δt . Also, Figure 7(a) illustrates the development of the Gaussian initial condition into solitary waves. As it is seen from the Figure 7(a), a solitary wave plus and oscillating tail are drawn. As seen from the figures, two solitary waves moving is observed. Contour line for evolution of solitary waves with Gaussian initial condition is depicted in Figure 7(b).

5.3.2. Undular bore initial condition

Production of a train of solitary waves is studied on Kudryashov-Sinelshchikov equation using the undular bore initial condition

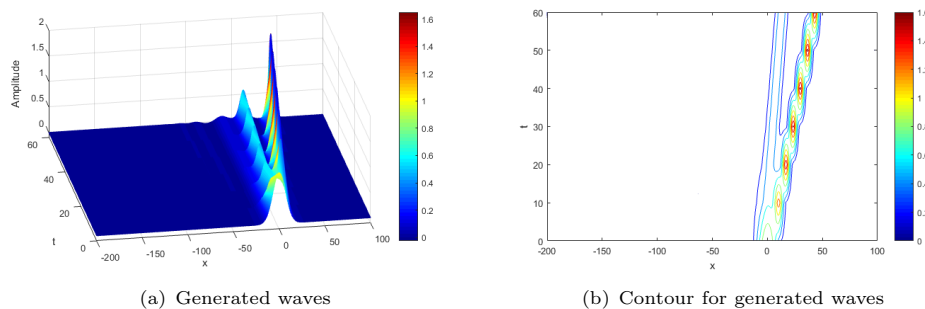
$$u(x, 0) = \frac{1}{2}u_0 \left[1 - \tanh\left(\frac{|x| - x_0}{d}\right) \right], \quad (5.9)$$

and boundary condition

$$u(-200, t) = u(100, t) = 0, \quad t > 0. \quad (5.10)$$

Table 4. Conserved quantities for evolution of solitary waves with Gaussian initial condition

t	$h = 0.1$	$\Delta t = 0.1$	$h = 0.08$	$\Delta t = 0.05$
	C_1	C_2	C_1	C_2
0	17.7245287586	-51.2261857478	17.7245503786	-51.2235091657
10	17.7245287586	-51.2301483544	17.7245503786	-51.2274731214
20	17.7245287590	-51.2373589096	17.7245503794	-51.2346847042
30	17.7245287628	-51.2402881706	17.7245503686	-51.2376138049
40	17.7245286775	-51.2411146178	17.7245502309	-51.2384401312
50	17.7245288162	-51.2413679672	17.7245503395	-51.2386934360
60	17.7245330256	-51.2414655930	17.7245544406	-51.2387910582

**Figure 7.** Generated waves and its contour for Gaussian initial condition

The undular bore refers the elevation of the water above the equilibrium surface at time $t = 0$. The changing in amplitude is centered on $x = x_0$ and the steepness of the change is measured by d . The values of d is inversely proportional to the steepness. The parameters are chosen as $u_0 = 1$, $x_0 = 25$ and $d = 5$ in Eq. (5.9).

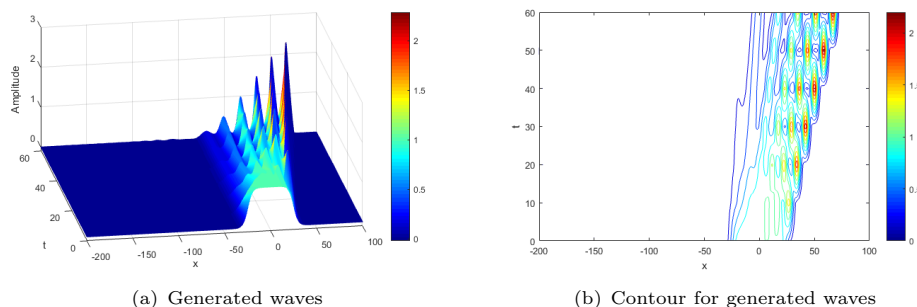
Choosing the parameters $\alpha = 1.5$, $\beta = 1.7$, $\gamma = 0.8$, $\sigma = -2.4$, $c = 0.425$, $\kappa = 1$, $\mu = 0.5$ for $h = \Delta t = 0.1$ and $h = \Delta t = 0.025$, the computational work is done up to $t = 60$. Variation of the conserved quantities C_1 and C_2 position is recorded in Table 5. Especially, the conserved quantity C_1 is preserved better for small values of h and Δt . Undulation bore keeps steady-state during running the which can be observed at specified times in Figure 8(a) and contour line for evolution of solitary waves with undular bore initial condition is shown in Figure 8(b). As it is seen from these figures, the initial perturbation evolves into a good developed train of solitary waves. As the time progresses, five solitary waves moving is observed.

6. Conclusion

Polynomial and rational wave solutions of Kudryashov-Sinelshchikov equation and numerical simulations for its dynamic motions have been studied. Conservation quantities of the dynamic motion have been calculated using multiplier approach. A collection of exact solitary and soliton solutions of Kudryashov-Sinelshchikov equation has been derived. Collocation finite element method based on quintic B-spline functions has been applied to the equation. The numerical scheme has been

Table 5. Conserved quantities for evolution of solitary waves with undular bore initial condition

t	$h = 0.1$	$\Delta t = 0.1$	$h = 0.25$	$\Delta t = 0.25$
	C_1	C_2	C_1	C_2
0	50.0001143360	-47.5406405155	50.0002271836	-47.5606776333
10	50.0001143358	-47.5472542687	50.0002271800	-47.5672722389
20	50.0001136922	-47.5669315179	50.0002273206	-47.5868910697
30	50.0001005086	-47.5859019717	50.0002283411	-47.6058195294
40	50.0001424769	-47.5972898726	50.0002113808	-47.6172077980
50	50.0001847283	-47.6029921696	50.0001054225	-47.6229362420
60	49.9999339684	-47.6057580275	50.0000515661	-47.6256782478

**Figure 8.** Generated waves and its contour for undular bore initial condition

shown to be unconditionally stable. To demonstrate the accuracy of the proposed method, we have considered three test problems including the motion of single solitary wave, interaction of two solitary waves and evolution of waves with Gaussian and undular bore initial conditions. Then, analytical and numerical results have been compared by aid of error norms. The obtained analytical and numerical results are in good agreement. The results of this paper come with a lot of encouragement for further future investigations.

References

- [1] H. I. Abdel-Gawad, M. Tantawy and M.S. Osman, *Dynamic of DNA's possible impact on its damage*, Mathematical Methods in the Applied Sciences, 2016, 39(2), 168–176.
- [2] M. N. Ali, S. Ali, S. M. Husnine and T. Ak, *Nonlinear self-adjointness and conservation laws of KdV equation with linear damping force*, Applied Mathematics & Information Sciences Letters, 2017, 5(3), 89–94.
- [3] M. N. Ali, A. R. Seadawy, S. M. Husnine and K.U. Tariq, *Optical pulse propagation in monomode fibers with higher order nonlinear Schrödinger equation*, Optik, 2018, 156, 356–364.
- [4] M. N. Ali, S. M. Husnine, S. Noor and A. Tuna, *Exact solutions of $(n + 1)$ -dimensional space-time fractional Zakharov-Kuznetsov equation*, Hittite Journal of Science and Engineering, 2018, 5(3), 179–183.

- [5] M. N. Ali, S. M. Husnine, T. Ak and A. Atangana, *Solitary wave solution and conservation laws of higher dimensional Zakharov-Kuznetsov equation with nonlinear self-adjointness*, Mathematical Methods in the Applied Sciences, 2018, 41, 6611–6624.
- [6] M. N. Ali, S. M. Husnine, A. Saha, S. K. Bhowmik, S. Dhawan and T. Ak, *Exact solutions, conservation laws, bifurcation of nonlinear and supernonlinear traveling waves for Sharma-Tasso-Olver equation*, Nonlinear Dynamics, 2018, 94, 1791–1801.
- [7] M. N. Ali, A. R. Seadawy and S. M. Husnine, *Lie point symmetries, conservation laws and exact solutions of $(1 + n)$ -dimensional modified Zakharov-Kuznetsov equation describing the waves in plasma physics*, Pramana-Journal of Physics, 2018, 8, 1054–1060.
- [8] S. C. Anco and G. Bluman, *Direct construction method for conservation laws of partial differential equations Part I: Examples of conservation law classifications*, European Journal of Applied Mathematics, 2002, 13(5), 545–566.
- [9] I. M. Anderson and J. Pohjanpelto, *The cohomology of invariant variational bicomplexes*, Acta Applicandae Mathematicae, 1995, 41, 3–19.
- [10] M. S. Bruzón, E. Recio, R. de la Rosa and M. L. Gandarias, *Local conservation laws, symmetries, and exact solutions for a Kudryashov-Sinelshchikov equation*, Mathematical Methods in the Applied Sciences, 2018, 41(4), 1631–1641.
- [11] B. Feng and T. Mitsui, *A finite difference method for the Korteweg-de Vries and the Kadomtsev-Petviashvili equations*, Journal of Computational and Applied Mathematics, 1998, 90(1), 95–116.
- [12] N. H. Ibragimov, *CRC Handbook of Lie Group Analysis of Differential Equations, Volume I: Symmetries, Exact Solutions, and Conservation Laws*, CRC Press, Boca Raton, 1993.
- [13] M. Inc, A. I. Aliyu, A. Yusuf and D. Baleanu, *Optical solitons for Biswas-Milovic model in nonlinear optics by Sine-Gordon equation method*, Optik-International Journal for Light and Electron Optics, 2018, 157, 267–274.
- [14] E. Noether, *Invariant and variation problems*, Transport Theory and Statistical Physics, 1971, 1(3), 186–207.
- [15] P. Olver, *Application of Lie Groups to Differential Equations*, Springer-Verlag, New York, 1986.
- [16] M. S. Osman, *Analytical study of rational and double-soliton rational solutions governed by the KdV-Sawada-Kotera-Ramani equation with variable coefficients*, Nonlinear Dynamics, 2017, 89(3), 2283–2289.
- [17] M. S. Osman and J.A. Machado, *The dynamical behavior of mixed-type soliton solutions described by $(2 + 1)$ -dimensional Bogoyavlensky-Konopelchenko equation with variable coefficients*, Journal of Electromagnetic Waves and Applications, 2018, 32(11), 1457–1464.
- [18] M. S. Osman, J.A.T Machado and D. Baleanu, *On nonautonomous complex wave solutions described by the coupled Schrödinger-Boussinesq equation with variable-coefficients*, Optical and Quantum Electronics, 2018, 50(2), 73.
- [19] M. S. Osman, A. Korkmaz, H. Rezazadeh, M. Mirzazadeh, M. Eslami and Q. Zhou, *The unified method for conformable time fractional Schrödinger equation with perturbation terms*, Chinese Journal of Physics, 2018, 56(5), 2500–2506.

- [20] P. M. Prenter, *Splines and Variational Methods*, John Wiley, New York, 1975.
- [21] M. Randrüüt, *On the Kudryashov-Sinelshchikov equation for waves in bubbly liquids*, Physics Letters A, 2011, 375(42), 3687–3692.
- [22] H. Stephani, *Differential Equations: Their Solution Using Symmetries*, Cambridge University Press, Cambridge, 1989.
- [23] H. Triki, T. Ak, S. P. Moshokoa and A. Biswas, *Soliton solutions to KdV equation with spatio-temporal dispersion*, Ocean Engineering, 2018, 91, 48.
- [24] M. Vlieg-Hulstman, *The Painlevé analysis and exact travelling wave solutions to nonlinear partial differential equations*, Mathematical and Computer Modelling, 1993, 18(10), 151–156.
- [25] A. M. Wazwaz, *The variational iteration method: A reliable analytic tool for solving linear and nonlinear wave equations*, Computers & Mathematics with Applications, 2007, 54(7–8), 926–932.
- [26] A. M. Wazwaz, *The Hirota's bilinear method and the tanh-coth method for multiple-soliton solutions of the Sawada-Kotera-Kadomtsev-Petviashvili equation*, Applied Mathematics and Computation, 2008, 200(1), 160–166.
- [27] H. Wu, *On Bäcklund transformations for nonlinear partial differential equations*, Journal of Mathematical Analysis and Applications, 1995, 192(1), 151–179.
- [28] H. Yang, *Symmetry reductions and exact solutions to the Kudryashov-Sinelshchikov equation*, Zeitschrift für Naturforschung A, 2016, 71(11)a, 1059–1065.
- [29] V. E. Zakharov and A.B. Shabat, *Interaction between solitons in a stable medium*, Soviet Physics-Journal of Experimental and Theoretical Physics, 1973, 37(5), 823–828.
- [30] S. Zhang and S. Hong, *Variable separation method for a nonlinear time fractional partial differential equation with forcing term*, Journal of Computational and Applied Mathematics, 2018, 339, 297–305.